

Generalized spheroidal wave equation for real and complex valued parameters. An algorithm based on the analytic derivatives for the eigenvalues

Mykhaylo V. Khoma

Max Planck Institute for the Physics of Complex Systems,

Nöthnitzer Str. 38, Dresden-01187, Germany

Institute of Electron Physics, National Academy of Sciences of Ukraine, Uzhhorod, Ukraine

(Dated: March 25, 2025)

Abstract

This paper presents a new approach for computations of eigenvalues of the generalized spheroidal wave equations. The novelty of the present method is in the use of the analytical derivatives of the eigenvalues to minimize losses in accuracy. The derivatives are constructed in the form of three-term recurrent relations within the method of continued fractions associated with the corresponding spheroidal wave equation.

Very accurate results for the eigenvalues are obtained for a wide range of the parameters of the problem. As an illustrative example, the electronic energies and the separation constants are computed for various electronic states and geometries of selected (H_2^+ , HeH^{2+} , and BH^{5+}) quasimolecular systems. We also presented the solutions of the eigenvalues for complex parameters of the generalized spheroidal wave equations. The agreement between the obtained results and the results of other authors is discussed.

I. INTRODUCTION

Generalized spheroidal wave equations (GSWEs) play a fundamental role in many research areas such as atomic and molecular physics [1–9], signal processing and electrodynamics [10–13], gravitation and cosmology [14–16], etc. Several approaches to determine the solutions for the GSWEs have been proposed in the literature [16–33].

However, despite many efforts, methods of solution for these equations certainly need further development. This seems to be related to the fact that the standard algorithms for their evaluation encounter numerical difficulties in practical computations for very large or complex valued parameters of the GSWE, as was noted in [32–36]. Finding efficient algorithms to compute GSWEs is still an area of ongoing research and a number of new studies have appeared in recent years [37–41].

The approach to solving the GSWEs boils down to finding their eigenvalues via non-linear search algorithms starting from (sufficiently good) initial guesses. The difficulty mostly resides in finding such good trial eigenvalues for their subsequent non-linear refinement. In the present study we eliminate this difficulty by using analytical derivatives of the sought-for eigenvalues with respect to the distance R between the foci of the spheroidal system of coordinates and the boundary conditions at $R = 0$.

Perhaps the most notable example of the application of GSWEs is the two-Coulomb-center problem eZ_1Z_2 , i.e., the problem of solving the Schrödinger equation for the motion of an electron in the field of two Coulomb centers with charges Z_1 and Z_2 at a fixed distance R from each other. In fact, mathematically the two-Coulomb-center problem is equivalent to two coupled GSWEs [16, 32, 42]. This paper is concerned with the accurate numerical solutions of GSWEs and applications of such solutions to the eZ_1Z_2 problem.

The structure of the paper is the following. We provide the necessary mathematical preliminaries and formulate the problem in Sec. II. In Sec. III we present the main mathematical result of this work, viz., analytic representations for the derivatives of the eigenvalues of the eZ_1Z_2 problem with respect to the internuclear distance. These analytical derivatives are used in Sec. IV in numerical calculations for the eZ_1Z_2 problem, including the symmetric H_2^+ and asymmetric (HeH^{2+} and BH^{5+}) cases. In the same section we present our results for the highly excited electronic energy of H_2^+ and very large internuclear distances ($\sim 10^5$ au). Continuum electronic states for eZ_1Z_2 problem are considered in subsection IV C. Calcula-

tions of the eigenvalues for complex valued parameters are presented in subsection IV D. We conclude in Sec. V. In the appendix we provide auxiliary information for section II.

Unless otherwise stated, atomic units ($\hbar = m_e = e = 1$) are used throughout this paper.

II. FORMULATION OF THE PROBLEM

A. The GSWE and the two-Coulomb-center problem

The generalized spheroidal wave equation can be given in the following form [16]:

$$t(t - t_0) \frac{\partial^2 y}{\partial t^2} + (B_1 + B_2 t) \frac{\partial y}{\partial t} + [\omega^2 t(t - t_0) - 2\alpha\omega(t - t_0) + B_3]y = 0, \quad (1)$$

where B_1 , B_2 , B_3 , α , ω , and t_0 are constants. The intervals of the independent variable t interesting for physical applications are both $[0 \leq t \leq t_0]$ and $[t_0 \leq t < \infty)$.

In view of application to the two-Coulomb-center problem, we use the prolate spheroidal coordinates (ξ, η, φ) . If Z_1 and Z_2 are the charges placed at a fixed distance R along a line defining the z axis and r_1 and r_2 are the distances of an electron from charges Z_1 and Z_2 , respectively, then ξ , η , and φ are defined as follows:

$$\begin{aligned} \xi &= (r_1 + r_2)/R, & \eta &= (r_1 - r_2)/R, & \varphi &= \arctan(y/x), \\ 1 &\leq \xi < \infty, & -1 &\leq \eta \leq 1, & 0 &\leq \varphi < 2\pi, \end{aligned} \quad (2)$$

where φ is the azimuthal angle with respect to the z axis. The Schrödinger equation for the eZ_1Z_2 problem reads

$$\nabla^2 \Psi + 2(E - V)\Psi(\vec{r}; R) = 0, \quad (3)$$

where $\Psi(\vec{r}; R)$ is the electronic wave function, $\vec{r} = (x, y, z)$ is the position vector of the electron, E is the electronic energy, and $V = -Z_1/r_1 - Z_2/r_2$ is the electron-nuclei potential. In the coordinates (2) the potential V reads

$$V = -\frac{2\xi Z_+}{R(\xi^2 - \eta^2)} - \frac{2\eta Z_-}{R(\xi^2 - \eta^2)}, \quad (4)$$

where $Z_+ = Z_1 + Z_2$ and $Z_- = Z_2 - Z_1$. For the sake of definiteness, we assume $Z_2 \geq Z_1$.

Owing to the form of the potential (4), equation (3) is separable in the prolate spheroidal coordinates (2). Therefore, the wave function Ψ can be factorized as follows:

$$\Psi(\vec{r}; R) = \Pi(\xi) \Xi(\eta) \frac{e^{\pm im\varphi}}{\sqrt{2\pi}}. \quad (5)$$

The functions $\Pi(\xi)$ and $\Xi(\eta)$ satisfy the following system of differential equations:

$$\left[L_\xi + \left(\lambda^{(\xi)} + c^2(\xi^2 - 1) + a\xi - \frac{m^2}{\xi^2 - 1} \right) \right] \Pi(\xi) = 0, \quad (6)$$

$$\left[L_\eta + \left(-\lambda^{(\eta)} + c^2(1 - \eta^2) + b\eta - \frac{m^2}{1 - \eta^2} \right) \right] \Xi(\eta) = 0, \quad (7)$$

where

$$L_\xi = \partial_\xi(\xi^2 - 1)\partial_\xi, \quad L_\eta = \partial_\eta(1 - \eta^2)\partial_\eta, \quad (8)$$

$$a = RZ_+, \quad b = RZ_-, \quad (9)$$

$c^2 = ER^2/2$, and $\lambda^{(\xi)}$, $\lambda^{(\eta)}$, and m are the separation constants (m is assumed to be a non-negative integer and is referred to as the modulus of the magnetic quantum number [21]). In the case $E < 0$ it is convenient to introduce the following parameters: $\varepsilon = \sqrt{-2E}$ and $p = \varepsilon R/2$.

Equations (6) and (7) are GSWEs. This can be demonstrated by using the substitutions $\Pi(\xi) = (\xi^2 - 1)^{m/2}f(\xi)$ and $\Xi(\eta) = (1 - \eta^2)^{m/2}g(\eta)$ for (6) and (7), respectively. The differential equations for $f(\xi)$ and $g(\eta)$ will take the form of equation (1) if we let $\xi = t - 1$ for the function $f(\xi)$ and $\eta = t - 1$ for the function $g(\eta)$, respectively [16, 32]. The parameters in (1) then read as follows: $t_0 = 2$, $\omega = c$, $\alpha = -R(Z_1 \pm Z_2)/2c$, $B_1 = -2(m+1)$, $B_2 = 2(m+1)$, and $B_3 = \lambda + m(m+1) + R(Z_1 \pm Z_2)$ (there is an apparent misprint in the last term of the expression for B_3 in [32]). Let us note here that the GSWE is also referred to as the confluent Heun equation (for details see [29, 30, 42]).

The form of Eqs. (6) and (7) is the most suitable for treating the continuum states. Here we first consider the discrete spectrum ($E < 0$) of the eZ_1Z_2 problem, which is described by Eqs. (6) and (7) subject to the formal substitution $c^2 \rightarrow -p^2$. The differential equations for $\Pi(\xi)$ and $\Xi(\eta)$ then reads

$$\left[L_\xi + \left(\lambda^{(\xi)} - p^2(\xi^2 - 1) + a\xi - \frac{m^2}{\xi^2 - 1} \right) \right] \Pi(\xi) = 0, \quad (10)$$

$$\left[L_\eta + \left(-\lambda^{(\eta)} - p^2(1 - \eta^2) + b\eta - \frac{m^2}{1 - \eta^2} \right) \right] \Xi(\eta) = 0. \quad (11)$$

The functions $\Pi(\xi)$ and $\Xi(\eta)$ satisfy the following boundary conditions:

$$|\Pi(1)| < \infty, \quad \lim_{\xi \rightarrow \infty} \Pi(\xi) = 0, \quad (12)$$

$$|\Xi(\pm 1)| < \infty. \quad (13)$$

Under the conditions (12) and (13) equations (10) and (11) each define a Sturm-Liouville problem with the spectral parameters $\lambda^{(\xi)}$ and $\lambda^{(\eta)}$, respectively [1]. The eigenfunctions and eigenvalues of the problem are characterized by the quantum numbers k and m for $\Pi_{km}(\xi)$ and $\lambda_{km}^{(\xi)}$, and q and m for $\Xi_{qm}(\eta)$ and $\lambda_{qm}^{(\eta)}$. The numbers k and q are equal to the numbers of nodes of the eigenfunctions $\Pi_{km}(\xi)$ and $\Xi_{qm}(\eta)$, respectively [19–21]. The quantum numbers (k, q, m) are related to the "united atom" quantum numbers (N, l, m) as follows: $N = k + q + m + 1$, $l = q + m$ ($0 \leq l \leq N - 1$, $0 \leq m \leq l$). The system of coupled equations (6) and (7) represents the solution of the Schrödinger equation (3) under the condition that the separation constants $\lambda_{km}^{(\xi)}$ and $\lambda_{qm}^{(\eta)}$ are equal:

$$\lambda_{km}^{(\xi)}(p, a) = \lambda_{qm}^{(\eta)}(p, b) \equiv \lambda. \quad (14)$$

Equation (14) possesses a unique solution for λ and p at fixed values of a and b (or, equivalently, R , Z_1 , and Z_2) and quantum numbers k , q , and m , i.e., $\lambda \equiv \lambda_{kqm}(R)$ and $p \equiv p_{kqm}(R)$. Usually, the $\lambda_{kqm}(R)$ and $p_{kqm}(R)$ are computed in an iterative manner starting from the known analytical expressions in the united atom limit:

$$\lambda_{kqm}(R \rightarrow 0) = -(q + m)(q + m + 1), \quad p_{kqm}(R \rightarrow 0) = 0. \quad (15)$$

Using the relation between p and E one obtains the discrete energy spectrum $E_{kqm}(R)$.

B. Expansions in series

The solutions to the equations (6) and (7) for the discrete spectrum are expanded in terms of some basis functions $u_s(\xi)$ and $v_s(\eta)$ as follows: $\Pi(\xi) = \sum_{s=0}^{\infty} c_s^{(\xi)} u_s(\xi)$ and $\Xi(\eta) = \sum_{s=0}^{\infty} c_s^{(\eta)} v_s(\eta)$. Substitution of these expansions into the equations for $\Pi(\xi)$ and $\Xi(\eta)$ lead to the following three-term recurrent relations for coefficients $c_s^{(\xi)}$ and $c_s^{(\eta)}$

$$\alpha_s^{(\xi, \eta)} c_{s+1}^{(\xi, \eta)} - \beta_s^{(\xi, \eta)} c_s^{(\xi, \eta)} + \gamma_s^{(\xi, \eta)} c_{s-1}^{(\xi, \eta)} = 0, \quad (16)$$

with boundary conditions $c_{-1}^{(\xi, \eta)} = 0$. The traditional choice for the radial basis $u_s(\xi)$ is due to Jaffe [43]:

$$\Pi(\xi) = (\xi^2 - 1)^{m/2} (\xi + 1)^\sigma e^{-p\xi} \sum_{s=0}^{\infty} c_s^{(\xi)} \left(\frac{\xi - 1}{\xi + 1} \right)^s, \quad (17)$$

where $\sigma = (a/2p) - m - 1$.

The angular basis $v_s(\eta)$ depends on the range of the internuclear distance R . For not very large distances ($R \lesssim 10$ a.u.) the expansion of $\Xi(\eta)$ in the associated Legendre functions $P_{s+m}^m(\eta)$ is used [1, 24]:

$$\Xi_{qm}(\eta) = (1 - \eta^2)^{m/2} e^{-p\eta} \sum_{s=0}^{\infty} c_s^{(\eta)} P_{s+m}^m(\eta). \quad (18)$$

For large R the expansion of $\Xi(\eta)$ in terms of $P_{s+m}^m(\eta)$ is found to converge badly [44]. In this case, one uses the following basis functions:

$$v_s^{\pm}(\eta) = (1 - \eta^2)^{m/2} \exp(\mp p\eta)(1 \pm \eta)^s. \quad (19)$$

For the computation of the eigenvalues both the v_s^+ and v_s^- are equivalent. For the computation of the wave functions, however, the basis v_s^- is preferred for the η -interval $[0, 1]$ and v_s^+ for the η -interval $[-1, 0]$, vice versa. The explicit form of coefficients $\alpha_s^{(\xi, \eta)}$, $\beta_s^{(\xi, \eta)}$, and $\gamma_s^{(\xi, \eta)}$ can be find elsewhere (see, e.g., [1, 16, 19–21] and references therein). For the sake of completeness we provide these coefficients in the appendix.

In the framework of the method of continued fractions (CFs) the eigenvalues $\lambda^{(\xi)}$ and $\lambda^{(\eta)}$ are calculated at fixed a and b by finding the roots of the following system of coupled characteristic equations [1, 16, 21, 32]:

$$\frac{F^{(\xi)}}{Q^{(\xi)}} \equiv \beta_0^{(\xi)} - \frac{\alpha_0^{(\xi)} \gamma_1^{(\xi)}}{\beta_1^{(\xi)} -} \frac{\alpha_1^{(\xi)} \gamma_2^{(\xi)}}{\beta_2^{(\xi)} -} \frac{\alpha_2^{(\xi)} \gamma_3^{(\xi)}}{\beta_3^{(\xi)} - \dots} = 0, \quad (20)$$

$$\frac{F^{(\eta)}}{Q^{(\eta)}} \equiv \beta_0^{(\eta)} - \frac{\alpha_0^{(\eta)} \gamma_1^{(\eta)}}{\beta_1^{(\eta)} -} \frac{\alpha_1^{(\eta)} \gamma_2^{(\eta)}}{\beta_2^{(\eta)} -} \frac{\alpha_2^{(\eta)} \gamma_3^{(\eta)}}{\beta_3^{(\eta)} - \dots} = 0. \quad (21)$$

Here $F^{(\xi, \eta)}$ and $Q^{(\xi, \eta)}$ are the numerators and denominators of the corresponding CF. Obviously, (20) and (21) are equivalent to the following equations:

$$F_{N_\xi}^{(\xi)}(p, a, \lambda^{(\xi)}) = 0, \quad (22)$$

$$F_{N_\eta}^{(\eta)}(p, b, \lambda^{(\eta)}) = 0. \quad (23)$$

In practice, CF is truncated at the (sufficiently large) N -th term. Here the subscripts N_ξ and N_η denote the number of terms (the length) of the corresponding CF. Expressions for $F_{N_\xi}^{(\xi)}$ and $F_{N_\eta}^{(\eta)}$ can be obtained by means of the recurrence relations [21, 45, 46]

$$F_j^{(\xi, \eta)} = \beta_j^{(\xi, \eta)} F_{j-1}^{(\xi, \eta)} - \alpha_{j-1}^{(\xi, \eta)} \gamma_j^{(\xi, \eta)} F_{j-2}^{(\xi, \eta)}, \quad (24)$$

with boundary conditions $F_{-2}^{(\xi,\eta)} = 0$ and $F_{-1}^{(\xi,\eta)} = 1$. For brevity, further we omit the subscripts N_ξ and N_η in notations for $F_{N_\xi}^{(\xi)}$ and $F_{N_\eta}^{(\eta)}$. Where necessary these values will be specified explicitly.

The separation constants $\lambda^{(\xi)}$ and $\lambda^{(\eta)}$ and the parameter p must be so chosen to satisfy simultaneously equations (22) and (23) and condition (14) at fixed value of R and quantum numbers k, q, m . The electronic energy E is found directly from the parameter p .

Solving system of Eqs. (22) and (23) involves a nonlinear root finding using, e.g., the Newton-Raphson algorithm, which starts from some trial values \bar{p} and $\bar{\lambda}$. The bottleneck of this approach is that the method is rather demanding of the quality of these trial parameters. The straightforward application of the root search routines, even for the one-dimensional case related to the continuum spectra of the problem, becomes very impractical for large parameters c, l , and m [32]. The situation is even more complex for two-dimensional case of the system of equations (22) and (23).

Another method, due to Hunter and Pritchard [19] and Hodge [20], consists of direct diagonalization of the matrix equation obtained from the three-term recurrence relations in Eq. (24). However, as was noted in Refs. [32, 33], this method is also inefficient for obtaining highly accurate eigenvalues. The method of Killingbeck [7, 8] also relies strongly on the availability of sufficiently accurate trial eigenvalues (see discussion in [32]).

In this work we propose a new way of obtaining high-precision eigenvalues of the eZ_1Z_2 problem (and related GSWEs) through accurate numerical integration of the system of coupled differential equations for $\lambda(R)$ and $p(R)$ [or $\lambda(R)$ and $E(R)$] with the boundary conditions (15). The needed analytical expressions for the derivatives $\frac{d\lambda(R)}{dR}$, $\frac{dE(R)}{dR}$, and $\frac{dp(R)}{dR}$, will be constructed in the next section. We note that λ , p , and E are smooth functions of R , and hence we can safely use a high-order numerical algorithm for the present task. The resulting eigenvalues are then used as starting guesses for the Newton-Raphson refinement.

III. DERIVATION OF THE EQUATIONS FOR dE/dR , dp/dR , AND $d\lambda/dR$

In this section we derive the expressions for $\frac{dE(R)}{dR}$, $\frac{dp(R)}{dR}$, and $\frac{d\lambda(R)}{dR}$ employing the chain rule and implicit differentiation methods. For the sake of brevity we have omitted the indices k, q , and m in notations for E_{kqm} , p_{kqm} , and λ_{kqm} . We adopt the following abbreviations

for the partial derivatives with respect to the arbitrary variable x , i.e.:

$$F_x^{(\xi,\eta)} \equiv \frac{\partial F^{(\xi,\eta)}}{\partial x}, \quad \lambda_x^{(\xi,\eta)} \equiv \frac{\partial \lambda^{(\xi,\eta)}}{\partial x}. \quad (25)$$

Let us start from the derivation of the expression for $\frac{dE(R)}{dR}$. The full differentials of the functions $F^{(\xi)}(p, a, \lambda)$ and $F^{(\eta)}(p, b, \lambda)$ with respect to the independent variable R reads

$$dF^{(\xi)} = \left(\frac{\varepsilon}{2} F_p^{(\xi)} + Z_+ F_a^{(\xi)} + F_\lambda^{(\xi)} \lambda_R^{(\xi)} \right) dR, \quad (26)$$

$$dF^{(\eta)} = \left(\frac{\varepsilon}{2} F_p^{(\eta)} + Z_- F_b^{(\eta)} + F_\lambda^{(\eta)} \lambda_R^{(\eta)} \right) dR. \quad (27)$$

In computation of the $dF^{(\xi)}$ and $dF^{(\eta)}$ we have used the explicit dependence of the variables a , b , and p on R (see section II A).

By equating $dF^{(\xi)}$ and $dF^{(\eta)}$ to zero [see Eqs. (22) and (23)] we obtain directly from (26) and (27)

$$\lambda_R^{(\xi)} = \left(F_\lambda^{(\xi)} \right)^{-1} \left(-\frac{\varepsilon}{2} F_p^{(\xi)} - Z_+ F_a^{(\xi)} \right), \quad (28)$$

$$\lambda_R^{(\eta)} = \left(F_\lambda^{(\eta)} \right)^{-1} \left(-\frac{\varepsilon}{2} F_p^{(\eta)} - Z_- F_b^{(\eta)} \right). \quad (29)$$

In the same manner, we can represent the full differentials $dF^{(\xi)}$ and $dF^{(\eta)}$ with respect to the independent variable E , namely

$$dF^{(\xi)} = \left(-\frac{R}{2\varepsilon} F_p^{(\xi)} + F_\lambda^{(\xi)} \lambda_E^{(\xi)} \right) dE, \quad (30)$$

$$dF^{(\eta)} = \left(-\frac{R}{2\varepsilon} F_p^{(\eta)} + F_\lambda^{(\eta)} \lambda_E^{(\eta)} \right) dE, \quad (31)$$

which lead to the following relations:

$$\lambda_E^{(\xi)} = \frac{R}{2\varepsilon} F_p^{(\xi)} \left(F_\lambda^{(\xi)} \right)^{-1}, \quad (32)$$

$$\lambda_E^{(\eta)} = \frac{R}{2\varepsilon} F_p^{(\eta)} \left(F_\lambda^{(\eta)} \right)^{-1}. \quad (33)$$

By taking the full differential of the expression (14) with respect to the independent variables E and R , we obtain (as the derivative of an implicit function)

$$\frac{dE_{kqm}}{dR} = \left(\lambda_R^{(\xi)} - \lambda_R^{(\eta)} \right) \left(\lambda_E^{(\eta)} - \lambda_E^{(\xi)} \right)^{-1}. \quad (34)$$

Substituting now Eqs. (28), (29), (32), and (33) into Eq. (34), we arrive at the final result for the derivative $\frac{dE_{kqm}}{dR}$, namely

$$\frac{dE(E, \lambda, R)}{dR} = \frac{\varepsilon^2}{R} + \frac{2\varepsilon \left(Z_- F_b^{(\eta)} F_\lambda^{(\xi)} - Z_+ F_a^{(\xi)} F_\lambda^{(\eta)} \right)}{R \left(F_p^{(\eta)} F_\lambda^{(\xi)} - F_p^{(\xi)} F_\lambda^{(\eta)} \right)}. \quad (35)$$

In numerical applications, however, it is more practical to use a pair of the derivatives $\frac{d\lambda}{dR}$ and $\frac{dp}{dR}$. The expression for $\frac{dp}{dR}$ can be obtained in the same way, and is given by

$$\frac{dp(p, \lambda, R)}{dR} = \frac{Z_- F_b^{(\eta)} F_\lambda^{(\xi)} - Z_+ F_a^{(\xi)} F_\lambda^{(\eta)}}{F_p^{(\xi)} F_\lambda^{(\eta)} - F_p^{(\eta)} F_\lambda^{(\xi)}}. \quad (36)$$

In a similar manner we can obtain the derivative $\frac{d\lambda}{dR}$. Again, let us write the full differentials $dF^{(\xi)}$ and $dF^{(\eta)}$ of the functions $F^{(\xi)}(p, a, \lambda)$ and $F^{(\eta)}(p, b, \lambda)$ in a general form:

$$dF^{(\xi)} \equiv F_p^{(\xi)} dp + F_a^{(\xi)} da + F_\lambda^{(\xi)} d\lambda = 0, \quad (37)$$

$$dF^{(\eta)} \equiv F_p^{(\eta)} dp + F_b^{(\eta)} db + F_\lambda^{(\eta)} d\lambda = 0. \quad (38)$$

From Eq. (37) it follows that

$$dp = - \left(F_a^{(\xi)} da + F_\lambda^{(\xi)} d\lambda \right) (F_p^{(\xi)})^{-1}, \quad (39)$$

which after substitution into Eq. (38) leads to an auxiliary relation

$$\frac{F_p^{(\eta)}}{F_p^{(\xi)}} (F_a^{(\xi)} Z_+ dR + F_\lambda^{(\xi)} d\lambda) = F_b^{(\eta)} Z_- dR + F_\lambda^{(\eta)} d\lambda. \quad (40)$$

From the relation (40) we finally obtain

$$\frac{d\lambda(p, \lambda, R)}{dR} = \frac{Z_+ F_p^{(\eta)} F_a^{(\xi)} - Z_- F_b^{(\eta)} F_p^{(\xi)}}{F_\lambda^{(\eta)} F_p^{(\xi)} - F_p^{(\eta)} F_\lambda^{(\xi)}}. \quad (41)$$

Thus, we obtained a system of the first-order differential equations (36) and (41) (or, alternatively, (35) and (41)). Solving this system is equivalent to finding the eigenvalues p_{kqm} and λ_{kqm} of the GSWEs (10) and (11).

IV. DETAILS OF NUMERICAL COMPUTATIONS AND EXAMPLES

To illustrate the proposed algorithm, we have computed the electronic energies and separation constants for the problem eZ_1Z_2 and represented here some examples. To compute $p_{kqm}(R)$ and $\lambda_{kqm}(R)$, we solve the system of algebraic equations (22) and (23) by a Newton-Raphson method [47] with the initial guesses \bar{p} and $\bar{\lambda}$ provided by solving the system of differential equations (36) and (41) at each propagation step of R . The numerical solution of the system of equations (36) and (41) obtained by using the 9th order explicit Runge-Kutta

method [48]. The Newton-Raphson refinement require the knowledge of the Jacobian of the system (see Chapter 9.6 of [47])

$$J = \begin{vmatrix} F_p^{(\xi)} & F_\lambda^{(\xi)} \\ F_p^{(\eta)} & F_\lambda^{(\eta)} \end{vmatrix}. \quad (42)$$

The required expressions for $F_{p,\lambda}^{(\xi,\eta)}$ were computed by means of explicit analytic differentiation of the corresponding recurrence relations (24). In all our computations, we set N_ξ and N_η to be equal ($N_\xi = N_\eta$). Going further, we denote by N_{RK} and N_{NR} the lengths of the continued fractions used for the Runge-Kutta propagation and for the Newton-Raphson refinement, respectively. For quantum numbers $(k, q) \leq 5$ and for the internuclear distances in the range $0.01 \leq R \leq 10$ a.u., it is enough to set $N_{\text{RK}} = 80$ and $N_{\text{NR}} = 160$ to ensure an accuracy of at least 28 digits for the E_{kqm} and λ_{kqm} . In the present calculations, we have chosen to use $N_{\text{RK}} = 100$ and $N_{\text{NR}} = 300$, except stated explicitly. Also we set $\Delta R = 0.01$ a.u. for the Runge-Kutta step in R . Three, or at most four Newton steps, were sufficient to achieve the desired accuracy for all computations in this work. The present algorithm has been implemented in FORTRAN-90 language. All computations of eigenvalues are carried out in quadruple precision arithmetic.

A. Hydrogen molecular ion H_2^+

One of the important applications of GSWEs is the study of the hydrogen molecular ion H_2^+ , which plays a fundamental role in quantum chemistry, plasma physics, atomic scattering theory, astrophysics, and astronomical spectroscopy [49–53], to cite a few. It further provides an excellent playground for testing a variety of numerical algorithms.

We have applied our method for computation of the electronic $E_{kqm}(R)$ and the Born-Oppenheimer (BO) potential energy curves (PECs) $E_{Nlm}^{\text{BO}}(R)$ for the ground and some excited electronic states of H_2^+ . We note that our results extend previous calculations in the literature. Here and further on we denote the BO PECs with a united atom notation for quantum numbers. The distance $R_0 = 2.0$ a.u. is used as a benchmark internuclear separation. As a test of the present algorithm we also calculated the equilibrium distances R_e (positions of the minimum of the BO PECs) for the electronic ground $1s\sigma_g$ and excited $2p\sigma_u$ and $3d\sigma_g$ states. To compute the R_e we gradually decrease the step in R , until the minimum was reached. For the $1s\sigma_g$ state we obtained $R_e = 1.997\ 193\ 319\ 969\ 9921$ a.u., which is

very close to the value of R_e reported in Ref. [50]. However, the corresponding BO energy: $-0.602\ 634\ 619\ 106\ 539\ 878\ 727\ 562\ 156\ 289\ 94$ is noticeably different from that reported in [50] which, since our results on electronic energies are otherwise in excellent agreement with earlier computations from the same authors and of Ishikawa in [49], we suspect is due to a misprint. We obtained the equilibrium distances of $R_e = 12.546\ 083\ 658\ 617\ 457$ a.u. with the BO energy: $-0.500\ 060\ 790\ 563\ 912\ 563\ 640\ 093\ 300\ 090\ 05$ a.u. for the $2p\sigma_u$ state, and $R_e = 8.834\ 164\ 503\ 179\ 2004$ a.u. with the BO energy: $-0.175\ 049\ 035\ 895\ 464\ 389\ 091\ 719\ 403\ 786\ 08$ a.u. for the $3d\sigma_g$ state. Numerical results are summarized in Table I (for the sake of compactness, we present the $E_{3d\sigma}^{\text{BO}}$ energy with fewer digits than it was reported in [50]).

1. The case of small R

It is well known that Jaffe's expansion for the radial solution $\Pi(\xi)$ converges slowly for very small R (see, e.g., Ref. [56] and references therein). Therefore, calculation of the electronic energies of H_2^+ at the small internuclear separations is a good test for the accuracy of the present method.

To verify our results we use an asymptotic (at $R \rightarrow 0$) representation for the energy of the $1s\sigma_g$ state. To the best of our knowledge, the most accurate asymptotic expression available for $\text{H}_2^+(1s\sigma_g)$ is the expansion to $O(R^{20})$ order obtained in Ref. [56], whose result ensures precision of at least 34 decimal digits for the electronic energy at the internuclear distances $\lesssim 0.005$ a.u. Our results and the result obtained from the asymptotic expansion of [56] are given in Table II. The computational time increases rapidly with increasing the number of terms N_{RK} and N_{NR} of the continued fractions. To provide some information about the overall computational cost, the total elapsed time, including the time for one step of Runge-Kutta propagation and three Newton-Raphson refinements, is also reported in Table II. Notice, however, that even for very moderate values of parameters N_{NR} and N_{RK} , the result is accurate to 10 decimal digits.

TABLE I. The electronic energies E_{kqm} and the BO energies E_{Nlm}^{BO} for the ground $1s\sigma_g$ and some excited states of H_2^+ computed at $R = 2.0$ a.u. and at specified equilibrium distances R_e . All values are given in atomic units (a.u.).

	R	energy
electronic state $1s\sigma_g$		
E_{000}	2.0	-1.102 634 214 494 946 461 508 968 945 318 34
Ref. [49]	2.0	-1.102 634 214 494 946 461 508 968 945
BO	R_e^{a}	-0.602 634 619 106 539 878 727 562 156 289 94
Ref. [50]	R_e^{b}	-0.602 634 619 106 539 869 378
electronic state $2s\sigma_g$		
E_{100}	2.0	-0.360 864 875 339 503 845 038 699 751 181 75
Ref. [54]	2.0	-0.360 864 875 339 503 845 038 699 8
electronic state $2p\sigma_u$		
E_{010}	2.0	-0.667 534 392 202 382 930 361 970 211 492 12
Ref. [49]	2.0	-0.667 534 392 202 382 930 361 970 211 49
BO	R_e^{c}	-0.500 060 790 563 912 563 640 093 300 090 05
Ref. [52]	R_e^{d}	-0.500 060 790 55
electronic state $2p\pi_u$		
E_{001}	2.0	-0.428 771 819 895 856 436 313 960 091 139 85
Ref. [54]	2.0	-0.428 771 819 895 856 436 313 960 1
electronic state $3p\sigma_u$		
E_{110}	2.0	-0.255 413 165 086 484 561 417 250 236 137 06
Ref. [54]	2.0	-0.255 413 165 086 484 561 417 250 2
electronic state $3d\sigma_g$		
BO	R_e^{e}	-0.175 049 035 895 464 389 091 719 403 786 08
Ref. [50]	R_e^{f}	-0.175 049 035 895 464 389 091 719 403 786 08
electronic state $4p\pi_u$		
BO	2.0	+0.384 084 709 963 404 777 081 630 847 953 27
Ref. [55]	2.0	+0.384 084 709 963

^a $R_e = 1.997\ 193\ 319\ 969\ 992\ 1$

^b $R_e = 1.997\ 193\ 319\ 969\ 992\ 9$

^c $R_e = 12.546\ 083\ 658\ 617\ 457$

^d $R_e = 12.545\ 25$

^e $R_e = 8.834\ 164\ 503\ 179\ 200\ 4$

^f $R_e = 8.834\ 164\ 503\ 179\ 200\ 609\ 421\ 533\ 521$

2. The case of large R

Calculation of the BO energies at large internuclear distances is also a good test for the accuracy. We computed the $E_{1s\sigma}^{\text{BO}}(R)$ energy of H_2^+ at a sufficiently large R and compared the

TABLE II. Convergence with increasing N_{RK} and N_{NR} of the electronic energy for the ground $1s\sigma_g$ state of H_2^+ at $R = 0.005$ a.u. The reference analytic asymptotic result from Ref. [56] is given at the bottom line of the table.

N_{RK}	N_{NR}	energy (a.u.)	CPU time (min:sec) ^a
10	20	-1.999 933 998 2	00:01
40	60	-1.999 933 998 24	00:01
100	200	-1.999 933 998 241 6	00:04
100	800	-1.999 933 998 241 654 7	00:40
100	2000	-1.999 933 998 241 654 732 489	04:04
100	4000	-1.999 933 998 241 654 732 490 695	17:26
100	8000	-1.999 933 998 241 654 732 490 695 394 316	64:28
100	9000	-1.999 933 998 241 654 732 490 695 394 316 08	81:25
Ref. [56]		-1.999 933 998 241 654 732 490 695 394 316 079	

^a Calculations were performed on a single core at 3.3 GHz.

results with the reference asymptotic values. The asymptotic expression for the degenerate at $R \rightarrow \infty$ energies of the $1s\sigma_g$ and $2p\sigma_u$ states of H_2^+ reads [57]

$$U(R) = -\frac{1}{2} - \frac{9}{4R^4} - \sum_{n=6}^{10} \frac{C_n}{R^n}, \quad (43)$$

where $C_6 = 15/2$, $C_7 = 213/4$, $C_8 = 7755/64$, $C_9 = 1773/2$, and $C_{10} = 86049/16$. As demonstrated in Table III, our calculations are in excellent agreement with the reference analytic results obtained from Eq. (43). Due to the asymptotic nature of the expansion (43), the values of $R \geq 2000$ a.u. are required to ensure the precision of at least 32 digits for Eq. (43). The exchange interaction, which decays exponentially at $R \rightarrow \infty$, can be totally neglected for such large values of R . Note the increasing values of $\Delta(R)$ (see Table III) with decreasing of R due to loss of precision of the asymptotic expansion (43). Table IV gives the present results for the BO energies and $\lambda_{Nlm}(R)$ for some excited states of H_2^+ at large internuclear distances compared to the reference values from Ref. [18]. For $R < 50$ a.u. we set $N_{\text{RK}} = 160$ and $N_{\text{NR}} = 600$, whereas for $R > 50$ a.u. we set $N_{\text{RK}} = 240$ and $N_{\text{NR}} = 1000$.

TABLE III. Convergence between the numerical $E_{1s\sigma}^{\text{BO}}(R)$ and the asymptotic $U(R)$ energies for the ground $1s\sigma_g$ state of H_2^+ with internuclear distance R . All values are given in atomic units. The numbers in parentheses denotes the powers of ten to be multiplied. Notation: $\Delta(R) = |E_{1s\sigma}^{\text{BO}}(R) - U(R)|$.

R	$E_{1s\sigma}^{\text{BO}}(R)$	$\Delta(R)$
800	-0.500 000 000 005 493 192 927 374 174 204 454	4.1(-28)
1000	-0.500 000 000 002 250 007 553 372 063 701 698	5.1(-29)
2000	-0.500 000 000 000 140 625 117 603 990 689 269	6.5(-32)
3000	-0.500 000 000 000 027 777 788 090 210 557 531	1.3(-33)

Solutions to the highly excited electronic states of H_2^+ at very large internuclear separation has been the subject of the quite recent study [53]. The comparison of the calculated BO potential minimum R_0 for selected $^2\Sigma$ electronic states is given in Table V. The overall agreement between the numbers is fairly well and is $\sim 0.5 - 0.03\%$. For the state ($q = 265$, $k = 2$) our data agree to better than $\sim 0.007\%$ with those reported in [53]. The computed potential energy curves for the considered electronic states are shown in Fig. 1.

The value $n_{\text{eff}}(R) = \sqrt{-2/E_{kqm}(R)}$ for the series of selected high-lying $^2\Sigma$ electronic states which undergo avoided crossings (i.e. with $k = 0$ and $q = n, n + 2, \dots$) is shown in Figures 2 and 3 for $q = 162 - 214$ and $q = 322 - 362$, respectively. Our computed BO potentials demonstrate the typical behavior of the avoided crossings (see e.g., Fig.2a of the Ref. [53]) which also serves as a criterion for the correctness of the obtained results. We note, that the present computation algorithm is stable and can be routinely extended to even higher quantum numbers.

TABLE IV. The BO energies $E_{Nlm}^{\text{BO}}(R)$ and the separation constants $\lambda_{Nlm}(R)$ for some excited electronic states of H_2^+ computed at large distances R . The numbers in parentheses denotes the powers of ten to be multiplied. All values are given in atomic units. The reference values are taken from Ref. [18].

state	R	E_{Nlm}^{BO} (Present/Ref. [18])/ λ_{Nlm} (Present/Ref. [18])
$3d\sigma_g$	50	-1.262 673 906 996 215 539 487 577 052 488(-1)
		-1.262 673 906 996(-1)
	90	-7.579 801 889 086 814 118 202 538 621 711(+1)
		-7.579 801 889 087(+1)
		-1.253 802 060 869 790 541 149 187 331 225(-1)
		-1.253 802 060 870(-1)
$5g\pi_g$	50	-1.358 934 082 084 459 026 365 146 867 789(+2)
		-1.358 934 082 084(+2)
	100	-5.737 246 183 910 849 059 533 104 430 085(-2)
		-5.737 246 183 911(-2)
		-6.954 309 290 022 620 755 949 470 218 992(+1)
		-6.954 309 290 023(+1)
	150	-5.600 302 812 696 510 402 376 796 685 615(-2)
		-5.600 302 812 697(-2)
		-1.368 102 002 800 595 095 361 298 816 688(+2)
		-1.368 102 002 801(+2)
		-5.575 405 175 595 630 988 817 932 376 624(-2)
		-5.575 405 175 596(-2)
		-2.036 608 739 009 452 820 868 095 110 508(+2)
		-2.036 608 739 009(+2)

TABLE V. Calculated position R_0 (a.u.) of the BO potential minimum of H_2^+ for selected highly excited $^2\Sigma$ electronic states in comparison with the data from Ref. [53].

state (q, k)	Ref. [53]	present
(189, 28)	46698	46360
(201, 30)	52646	52495
(237, 11)	62245	62226
(233, 17)	62709	62669
(265, 2)	73152	73147
(283, 0)	82444	82392

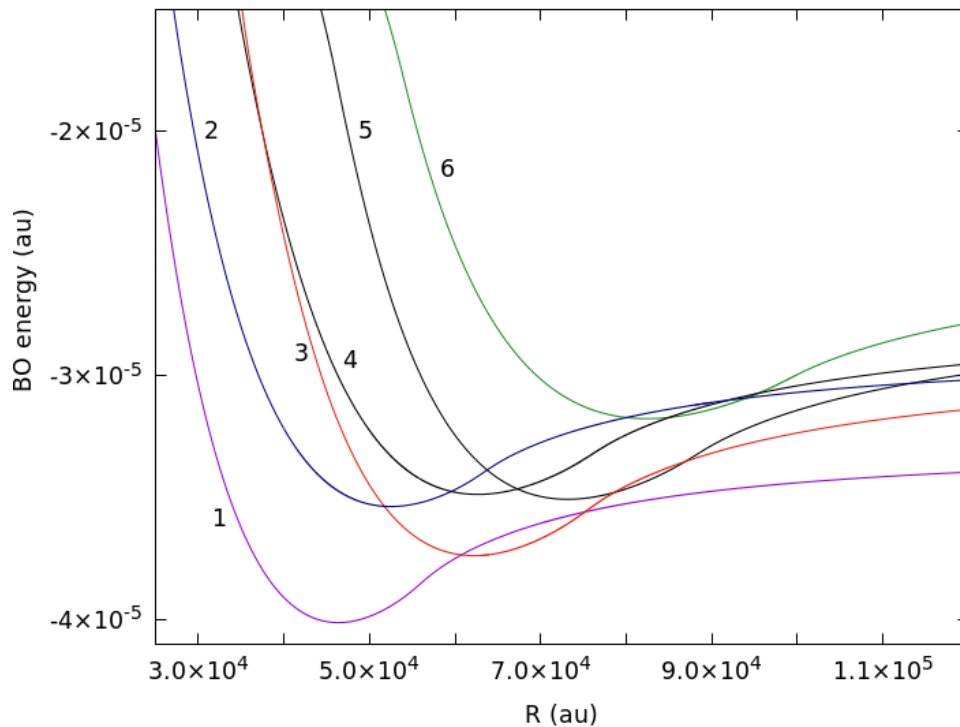


FIG. 1. PECs for selected highly excited states of H_2^+ (see also Table V): 1, $(q, k) = (189, 28)$; 2, $(q, k) = (201, 30)$; 3, $(q, k) = (237, 11)$; 4, $(q, k) = (233, 17)$; 5, $(q, k) = (265, 2)$; 6, $(q, k) = (283, 0)$.

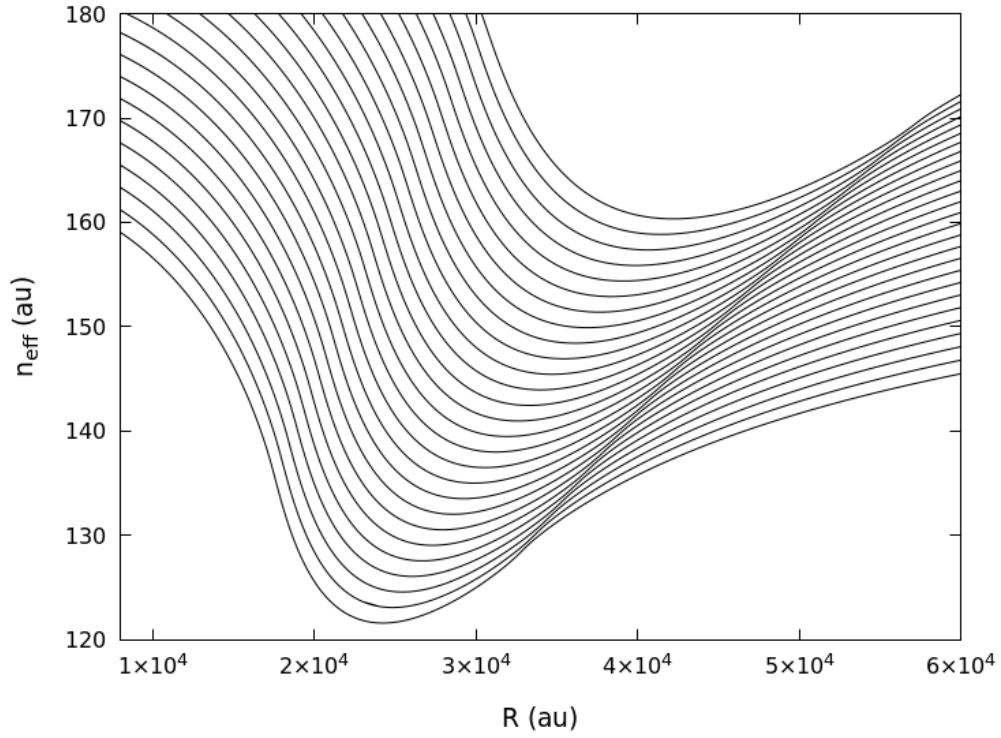


FIG. 2. Ridge of avoided crossings shown for states $(k, q, m) = (0, q, 0)$, $q = 162, 164, \dots, 214$.

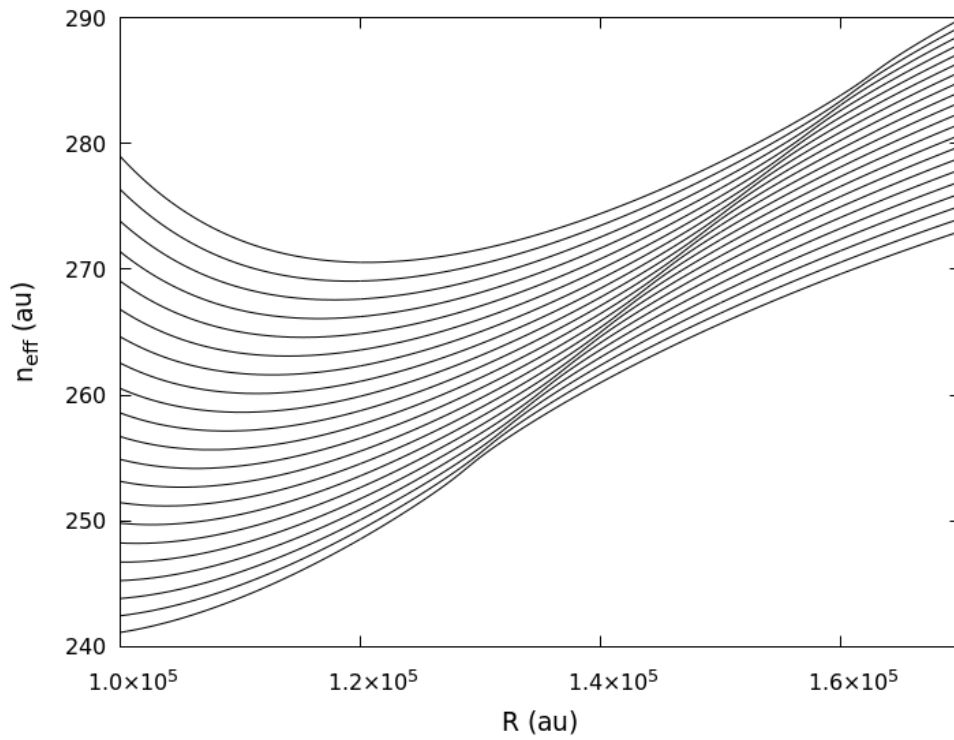


FIG. 3. The same as in Fig. 2 but for the states $q = 322, 324, \dots, 362$.

B. Exact Demkov's solution

It is known that there exist exact analytical solutions [58] of the eZ_1Z_2 problem for certain combinations of parameters Z_1 , Z_2 ($Z_1 \neq Z_2$), and R . We have used as a benchmark test a one such solution for the $3p\sigma$ state for $Z_1 = 1$, $Z_2 = 5$, and $R = \sqrt{10}/3$ a.u. We have reproduced the analytic results for the electronic energy, $E = -2$ a.u., and the separation constant, $\lambda = -10/3$, with the precision of 32 decimal digits by setting $N_{\text{RK}} = 40$ and $N_{\text{NR}} = 60$.

C. Continuum spectrum

The method presented here can also be applied to the computation of the continuum spectrum of the two-Coulomb-center problem, see Eqs. (6) and (7). In fact, its application is much simpler than the one for the bound spectrum. The problem is reduced to finding the eigenvalue (separation constant) $\lambda_{qm}(R)$ with the positive electronic energy E treated as a free parameter. In this case, expression (41) is simplified to

$$\begin{aligned} \frac{d\lambda_{qm}(R)}{dR} &= -F_R^{(\eta)}/F_\lambda^{(\eta)} \\ &= -\frac{Z_-F_b^{(\eta)} + (\kappa/2)F_c^{(\eta)}}{F_\lambda^{(\eta)}}, \end{aligned} \quad (44)$$

were $c = \kappa R/2$ and $\kappa = \sqrt{2E}$. For computation of the $F_R^{(\eta)}$, $F_\lambda^{(\eta)}$, $F_b^{(\eta)}$, and $F_c^{(\eta)}$, one can use the formulas (A.3) provided that the formal substitution, $p \rightarrow ic$, is made.

As an illustration, we present here the results of a calculation of the separation constant λ_{00} for the electronic continuum of HeH^{2+} ($Z_1 = 1$ and $Z_2 = 2$). The Runge-Kutta propagation has been carried out with $N_{\text{RK}} = 200$ and $\Delta R = 0.0005$ a.u. Clearly, the convergence of the numerical propagation is very good in the present one-dimensional case. Therefore, we did not employ a Newton-Raphson refinement. Our results for λ_{00} are compared to the results of [59] and given in Table VI. For the details on the construction of the continuum solution of the two-Coulomb-center problem we refer the readers to [22, 59].

TABLE VI. Calculated eigenvalue λ_{00} for the $s\sigma$ continuum state of HeH^{2+} ($l = 0, m = 0$) at $R = 1.0$ a.u. and for different values of κ compared with the data from Ref. [59]. All values are given in atomic units.

κ	λ_{00} (Present/Ref. [59])
0.2	-0.164 017 311 895 064 441 002 855 443 -0.164 017 311 895 064
1.0	-0.317 583 235 505 184 819 402 454 361 -0.317 583 235 505 185
5.0	-4.679 927 586 097 650 085 563 349 296 -4.679 927 586 097 65

D. Complex valued parameters

Solving the spheroidal wave equations with the complex valued parameters is a numerically difficult task [33, 36, 40]. However, the advantage of the present approach is that, it can be directly applied for calculation of the eigenvalues both for SWEs and GSWEs with complex parameters.

Our results of the calculations of eigenvalues for SWE (i.e. Eq. (7) with $b = 0$) for different c are presented in Tables VII and VIII and compared with the results reported in [33, 36, 40]. Overall, the present results are in better agreement with the data of [36] than those reported in a more recent study [40].

In Table IX we show the results of the present computation of the branch point c with corresponding eigenvalue $\lambda_{ml}(c)$ of SWE (7) compared with results of [36, 60].

TABLE VII. Eigenvalues $\lambda_{mn}(c)$ of SWE ($b = 0$) for real c^2 . Present work (PW)/[other authors].

m	n	c	Ref.	$-\lambda_{mn}(c)$	$\lambda_{mn}(ic)$
0	0	1	PW	0.68099 99448 53107 26021 60180 141	0.65139 76005 29730 91052 36276 172
0	0	10	PW	90.77169 57027 50054 84898 77312 426	18.97205 60550 42243 81391 0919
			[33]	90.77169 57027 50054 84898 77312	18.97205 60550 42243 81391 09191
0	0	100	PW	9900.75189 88910 16747 44954 21523 33	198.99747 46340 82502
			[33]	9900.75189 88910 16747 44954 21523	198.99747 46340 82548 13572 48103
1	1	1	PW ^a	2.19554 83554 13003 95688 27437 346	1.79530 45872 81818 78854 10816
			[36]	2.19554 8355	
			[40]	2.19561 23696 53500	
1	1	4	PW ^a	4.39959 30671 65506 10459 61890 349	-2.90920 07591 46191 61848 25064
			[36]	4.39959 3067	
			[40]	4.39959 97606 64940	
1	1	10	PW	89.71223 12326 08531 82924 20083 558	37.88064 98956 19453 22628 71048
			[33]	89.71223 12326 08531 82924 20083	37.88064 98956 19453 22628 71049
1	1	100	PW	9899.74682 23865 85061 62347 2435446	397.98984 67939 13
			[33]	9899.74682 23865 85061 62347 24354	397.98984 67939 13121 45974 40124
4	11	i	PW ^a	131.56008 09194 06941 64691 87548	
			[40]	131.56008 09183 03	

^a Result for $\lambda_{mn}(c) + c^2$

TABLE VIII. Values of the separation constants for SWE ($b = 0$) for $m = l = 0$. Present Work(PW)/[other authors]. Notation: $\alpha = 1 + i$.

c	Ref.	Re $[\lambda_{00}(c)]$	Im $[\lambda_{00}(c)]$
α	PW	0.05947 27697 35031 26247 06156 230	-1.33717 48778 05399 97103 72378 512
	[33]	0.05947 27697 35031 26247 06156	-1.33717 48778 05399 97103 72378
5α	PW	4.23035 06988 78380 87794 25891	-44.97310 67423 02780 62895 65852
10α	PW	9.24076 62146 34603 35159 57442 763	-189.98934 85956 57553 67515 08696 381
	[33]	9.24076 62146 34603 35159 57442	-189.98934 85956 57553 67515 08696
20α	PW ^a	19.24532 81345 43127 94480	20.00499 41449 70279 83195
	[40]	19.24532 81302 15245	20.00499 41471 04920

^a Result for $\lambda_{mn}(c) + c^2$

TABLE IX. Branch points c and the values of the separation constants $\lambda_{ml}(c)$. Present/Ref. [60]/Ref. [36].

m	l	c	$\lambda_{ml}(c)$
0	0,2	1.824 771 498 41 + 2.601 671 385 78 i	1.704 994 282 35 + 4.223 532 951 35 i
		1.824 770 + 2.601 670 i	1.705 180 + 4.220 186 i
		1.824 770 + 2.601 670 i	1.701 836 + 4.219 998 i
0	2,4	2.094 212 236 + 5.807 965 661 i	1.957 363 395 + 8.586 752 948 i
		2.094 267 + 5.807 965 i	1.998 518 + 8.578 716 i
		2.094 267 + 5.807 965 i	1.993 901 + 8.576 325 i

V. CONCLUDING REMARKS

We have presented an algorithm for solving the generalized spheroidal wave equations by employing the derivatives of the eigenvalues with respect to the distance R between the foci of the spheroidal system of coordinates. We have described how to evaluate these derivatives in analytic form within the method of continued fractions. As an application of the developed approach, we have performed calculations of the eigenvalues (electronic energies and separation constants) for the two-Coulomb-center problem for several benchmark geometries of the system. We have demonstrated the application of the method both for the discrete and continuum spectrum of the eZ_1Z_2 problem as well as to the solution for GSWEs with complex valued parameters. A representative set of results are presented and compared with the calculations of other authors. In the vast majority of cases, we obtained excellent agreement with the results of other authors, but in some cases a considerable disagreement is observed.

To conclude, we confirm that proposed algorithm is robust and can be used for an exceptionally wide range of the parameters of the problem. The accuracy of the method is very high and is actually limited by the accuracy of the employed computer arithmetic.

Appendix

The coefficients $\alpha_s^{(\xi)}$, $\beta_s^{(\xi)}$, and $\gamma_s^{(\xi)}$ for the expansion (17) reads

$$\begin{aligned}\alpha_s^{(\xi)} &= (s+1)(s+m+1), \\ \beta_s^{(\xi)} &= -\lambda^{(\xi)} + 2s(2p+s-\sigma) - 2p\sigma - (m+1)(m+\sigma), \\ \gamma_s^{(\xi)} &= \left(s - \frac{a}{2p}\right) \left(s - \frac{a}{2p} + m\right).\end{aligned}\tag{A.1}$$

The coefficients $\alpha_s^{(\eta)}$, $\beta_s^{(\eta)}$, and $\gamma_s^{(\eta)}$ for the expansion (18) reads

$$\begin{aligned}\alpha_s^{(\eta)} &= \frac{(s+2m+1)[b-2p(s+m+1)]}{2(s+m)+3}, \\ \beta_s^{(\eta)} &= \lambda^{(\eta)} + (s+m)(s+m+1), \\ \gamma_s^{(\eta)} &= \frac{s(b+2p(m+s))}{2(m+s)-1}.\end{aligned}\tag{A.2}$$

For the basis v_s^+ (see Eq. (19)) the coefficients $\alpha_s^{(\eta)}$, $\beta_s^{(\eta)}$, and $\gamma_s^{(\eta)}$ reads

$$\begin{aligned}\alpha_s^{(\eta)} &= 2(s+1)(s+m+1), \\ \beta_s^{(\eta)} &= \lambda^{(\eta)} + b + (2s+m+1)(2p+m) + s(s+1), \\ \gamma_s^{(\eta)} &= b + 2p(s+m).\end{aligned}\tag{A.3}$$

For the basis v_s^- the coefficients $\alpha_s^{(\eta)}$, $\beta_s^{(\eta)}$, and $\gamma_s^{(\eta)}$ are given by the same expressions (A.3), albeit with the substitution $b \rightarrow -b$.

ACKNOWLEDGMENTS

I thank Matt Eiles for valuable comments and recommendations for shaping the manuscript and to Eugen Yu. Remeta for many encouraging discussions. The Visitors Program Fellowship from the Max Planck Institute for the Physics of Complex Systems is greatly acknowledged. This study was partially supported by the U.S. Office of Naval Research Global (Grant N 62909-23-1-2088). The main part of the computations was undertaken with the assistance of resources from the National Computational Infrastructure (NCI), which is supported by the Australian Government in the framework of Ukraine-Australia Research Fund 2023.

-
- [1] R. K. Janev, L. P. Presnyakov, and V. P. Shevelko, *Physics of Highly Charged Ions* (Springer-Verlag, Berlin, 1985).
 - [2] J. M. Brown and A. Carrington, *Rotational Spectroscopy of Diatomic Molecules* (Cambridge University Press, Cambridge, 2003).
 - [3] V. Y. Lazur, M. V. Khoma, and R. K. Janev, *J. Phys. B: At. Mol. Phys.* **37**, 1245 (2004).
 - [4] D. I. Bondar, M. Hnatich, and V. Y. Lazur, *J. Phys. A: Math. Gen.* **40**, 1791 (2007).
 - [5] J. M. Rost, *Hyperfine Interact.* **89**, 343 (1994).
 - [6] M. L. Martiarena and V. H. Ponce, *Nucl. Instr. Meth. Phys. Res. B* **125**, 228 (1997).
 - [7] A. Yanacopoulo, G. Hadinger, and M. Aubert-Frecon, *J. Phys. B: At. Mol. Opt. Phys.* **22**, 2427 (1989).

- [8] G. Hadinger, M. Aubert-Frecon, and G. Hadinger, *J. Phys. B: At. Mol. Opt. Phys.* **22**, 697 (1989).
- [9] B. C. Eu and M. L. Sink, *J. Chem. Phys.* **78**, 4896 (1983).
- [10] T. Hrycak, S. Das, and G. Matz, *IEEE Transact. Signal Proc.* **60**, 2666 (2012).
- [11] A. Osipov, V. Rokhlin, and H. Xiao, *Prolate Spheroidal Wave Functions of Order Zero. Mathematical Tools for Bandlimited Approximation* (Springer, New York, 2013).
- [12] S. Deng, *Journal of Electrostatics* **66**, 549 (2008).
- [13] L.-W. Li, X.-K. Kang, and M.-S. Leong, *Spheroidal Wave Functions in Electromagnetic Theory* (John Wiley & Sons Inc., New York, 2002).
- [14] S. A. Teukolsky, *Class. Quantum Grav.* **32**, 124006 (2015).
- [15] P. P. Fiziev, *Class. Quantum Grav.* **27**, 135001 (2010).
- [16] E. W. Leaver, *J. Math. Phys.* **27**, 1238 (1986).
- [17] J. M. Peek, *J. Chem. Phys.* **43**, 3004 (1965).
- [18] M. M. Madsen and J. M. Peek, *Atomic Data* **2**, 171 (1971).
- [19] G. Hunter and H. O. Pritchard, *J. Chem. Phys.* **46**, 2146 (1967).
- [20] D. B. Hodge, *J. Math. Phys.* **11**, 2308 (1970).
- [21] J. D. Power, *Phil. Trans. R. Soc. A* **274**, 663 (1973).
- [22] J. Rankin and W. R. Thorson, *J. Comput. Phys.* **32**, 437 (1979).
- [23] L. I. Ponomarev and L. N. Somov, *J. Comput. Phys.* **20**, 183 (1976).
- [24] I. V. Komarov, L. I. Ponomarev, and S. Y. Slavyanov, *Spheroidal and Coulomb Spheroidal Functions* (Nauka, Moscow, 1976).
- [25] S. Y. Ovchinnikov and J. H. Macek, *Phys. Rev. A* **55**, 3605 (1997).
- [26] A. A. Abramov and S. V. Kurochkin, *Comput. Math. Math. Phys.* **46**, 10 (2006).
- [27] L. J. El-Jaick and B. D. Figueiredo, *Appl. Math. Comp.* **284**, 234 (2016).
- [28] B. D. B. Figueiredo, *J. Phys. A: Math. Gen.* **35**, 2877–2906 (2002).
- [29] B. D. B. Figueiredo, *J. Math. Phys.* **48**, 013503 (2007).
- [30] L. J. El-Jaick and B. D. B. Figueiredo, *J. Math. Phys.* **49**, 083508 (2008).
- [31] T. C. Scott, M. Aubert-Frécon, and J. Grotendorst, *Chem. Phys.* **324**, 323 (2006).
- [32] J. W. Liu, *J. Math. Phys.* **33**, 4026 (1992).
- [33] P. E. Falloon, P. C. Abbott, and J. B. Wang, *J. Phys. A: Math. Gen.* **36**, 5477 (2003).
- [34] D. Yan, L.-Y. Peng, and Q. Gong, *Phys. Rev. E* **79**, 036710 (2009).

- [35] P. Charles, *J. Phys. B: At. Mol. Opt. Phys.* **31**, 3621 (1998).
- [36] L. Li, M. Leong, T. Yeo, P. Kooi, and K. Tan, *Phys. Rev. E* **58**, 6792 (1998).
- [37] A. Singor, J. S. Savage, I. Bray, B. I. Schneider, and D. V. Fursa, *Comp. Phys. Comm.* **282**, 108514 (2023).
- [38] D. M. Mitnik, F. A. López, and L. U. Ancarani, *Mol. Phys.* **119**, e1881179 (2021).
- [39] M. Seri, *J. Math. Phys.* **56**, 012902 (2015).
- [40] D. X. Ogburn, C. L. Waters, M. D. Sciffer, J. A. Hogan, and P. C. Abbot, *Comp. Phys. Comm.* **185**, 244 (2014).
- [41] G. B. Cook and M. Zalutskiy, *Phys. Rev. D* **90**, 124021 (2014).
- [42] S. Y. Slavyanov and W. Lay, *Special functions* (Oxford University Press, Oxford, 2000).
- [43] G. Jaffe, *Z. Phys.* **87**, 535 (1934).
- [44] L. I. Ponomarev and T. P. Puzynina, *Zh. Vych. Mat. Mat. Fiz.* **8**, 1256 (1968).
- [45] W. Gautschi, *SIAM Rev.* **9**, 24 (1967).
- [46] H. S. Wall, *Analytic Theory of Continued Fractions* (Van Nostrand, New York, 1948).
- [47] W. Press, S. A. Teukolsky, W. Vetterling, and B. Flannery, *Numerical Recipes in FORTRAN: The Art of Scientific Computing*, 2nd ed. (Cambridge University Press, New York, 1992).
- [48] C. Tsitouras, *Appl. Numer. Math.* **38**, 123 (2001).
- [49] A. Ishikawa, H. Nakashima, and H. Nakatsuji, *J. Chem. Phys.* **128**, 124103 (2008).
- [50] H. Nakashima and H. Nakatsuji, *J. Chem. Phys.* **139**, 074105 (2013).
- [51] M. C. Zammit, J. S. Savage, J. Colgan, D. V. Fursa, D. P. Kilcrease, I. Bray, C. J. Fontes, P. Hakel, and E. Timmermans, *The Astrophys. Journ.* **851**, 64 (2017).
- [52] H. Olivares-Pilón and A. V. Turbiner, *Ann. Phys.* **373**, 581 (2016).
- [53] T. J. Price and C. H. Greene, *J. Phys. Chem. A* **122**, 8565 (2018).
- [54] P.-C. Li and S.-I. Chu, *Chin. Phys. B* **29**, 083202 (2020).
- [55] L. Tao, C. W. McCurdy, and T. N. Rescigno, *Phys. Rev. A* **79**, 012719 (2009).
- [56] B. Nickel, *J. Phys. A: Math. Theor.* **44**, 395301 (2011).
- [57] C. A. Coulson, *Proc. R. Soc. A* **61**, 20 (1941).
- [58] Y. N. Demkov, *JETP Letters* **7**, 101 (1968).
- [59] M. Hiyama and H. Nakamura, *Comp. Phys. Comm.* **103**, 209 (1997).
- [60] T. Oguchi, *Radio Sci.* **5**, 1207 (1970).